EARTHQUAKE ENGINEERING AND STRUCTURAL DYNAMICS
Earthquake Engng Struct. Dyn. 2004; **33**:35–48 (DOI: 10.1002/eqe.336)

Comparison of displacement coefficient method and capacity spectrum method with experimental results of RC columns

Yu-Yuan Lin[1,*,†], Kuo-Chun Chang[2] and Yuan-Li Wang[2]

[1]*Department of Civil and Environmental Engineering, Stanford University, Stanford, CA 94305, U.S.A.*
[2]*Department of Civil Engineering, National Taiwan University, Taipei 106, Taiwan*

SUMMARY

For the performance-based seismic design of buildings, both the displacement coefficient method used by FEMA-273 and the capacity spectrum method adopted by ATC-40 are non-linear static procedures. The pushover curves of structures need to be established during processing of these two methods. They are applied to evaluation and rehabilitation of existing structures. This paper is concerned with experimental studies on the accuracy of both methods. Through carrying out the pseudo-dynamic tests, cyclic loading tests and pushover tests on three reinforced concrete (RC) columns, the maximum inelastic deformation demands (target displacements) determined by the coefficient method of FEMA-273 and the capacity spectrum method of ATC-40 are compared. In addition, a modified capacity spectrum method which is based on the use of inelastic design response spectra is also included in this study. It is shown from the test specimens that the coefficient method overestimates the peak test displacements with an average error of +28% while the capacity spectrum method underestimates them with an average error of −20%. If the Kowalsky hysteretic damping model is used in the capacity spectrum method instead of the original damping model, the average errors become −11% by ignoring the effect of stiffness degrading and −1.2% by slightly including the effect of stiffness degrading. Furthermore, if the Newmark–Hall inelastic design spectrum is implemented in the capacity spectrum method instead of the elastic design spectrum, the average error decreases to −6.6% which undervalues, but is close to, the experimental results. Copyright © 2003 John Wiley & Sons, Ltd.

KEY WORDS: coefficient method; capacity spectrum method; evaluation; pseudo-dynamic test; cyclic loading test; pushover test

INTRODUCTION

After several destructive earthquakes in the past decade, a common consensus has been reached whereby the present seismic design codes of structures need to be essentially improved for

*Correspondence to: Yu-Yuan Lin, Visiting Scholar, Rm 556 H, Bldg 550, Department of Civil and Environmental Engineering, Stanford University, Stanford, CA 94305, U.S.A.
†E-mail: yylin@ncree.gov.tw

Contract/grant sponsor: National Science Council, Taiwan; contract/grant number: NSC-90-2811-Z-002-003
Contract/grant sponsor: Sinotech Engineering Consultant Inc., Taiwan; contract/grant number: 6120

Received 27 September 2002
Revised 3 February 2003
Accepted 18 April 2003

predicting structural responses. On the basis of the requirement, performance-based seismic engineering was developed. Currently, there are two well-known force–displacement seismic evaluation and rehabilitation methods. One is the coefficient method used in the FEMA-273 document [1] and the other is the capacity spectrum method adopted in the ATC-40 document [2].

FEMA-273, which was developed by the Federal Emergency Management Agency of the U.S.A., is a guideline for seismic rehabilitation of buildings. There are four seismic rehabilitation procedures proposed by this guideline to estimate whether structures meet the required performance or not. They are the linear static procedure, the linear dynamic procedure, the non-linear static procedure (also known as the coefficient method or displacement coefficient method) and the non-linear dynamic procedure. In this paper, only the coefficient method is discussed. The displacement demand of the method is determined from the elastic one by using a number of correction factors based on statistical analyses.

The capacity spectrum method (CSM) was first introduced by Freeman [3, 4] as a rapid evaluated procedure for assessing the seismic vulnerability of buildings. This procedure compares the structural capacity in the form of a pushover curve with demands on the structure in the form of an elastic response spectrum. The graphical intersection of the two curves approximates the response of the structure [3–7]. In order to account for the effects of non-linear behavior of structures, equivalent viscous damping has been implemented to modify the elastic response spectrum. Implied in the capacity spectrum method is that the maximum inelastic deformation demand of a non-linear single-degree-of-freedom (SDOF) system can be approximately estimated by an iterative procedure of a series of linear secant representation systems. Therefore, it avoids dynamic analysis of inelastic systems.

After the capacity spectrum method was adopted by ATC-40, Fajfar [8] and Chopra and Goel [9, 10] pointed out that the ATC-40 procedure significantly underestimated the deformation demands of systems for a wide range of periods when used for the Type A idealised hysteretic damping model. Improved methods were proposed by them by implementing the inelastic design response spectrum as the demand diagram of the capacity spectrum method. Notice that in actual practice, the ATC-40 procedure uses reduced Types B and C damping values for evaluating the existing reinforced concrete structures.

The purpose of this paper is to clarify the accuracy of the coefficient method and the capacity spectrum method by conducting the pseudo-dynamic tests, cyclic loading tests and pushover tests on three RC columns. The maximum top displacements measured from pseudo-dynamic tests will be taken as references to compare with those estimated from the evaluation methods. The force–displacement relationship obtained from pushover tests will be regarded as the pushover curves (i.e., the capacity curves) of the coefficient method and the capacity spectrum method to evaluate the target displacements of these specimens. In addition, the status of stiffness and strength degrading of the RC columns can be comprehended from cyclic loading tests.

THE TEST SPECIMENS

In the tests, triplicate RC columns are made (Figure 1) according to the direct displacement-based design procedure [11]. These specimens are designed primarily for studying that procedure. Their height and reaction weight (0.5 times self weight plus the weight of the supported

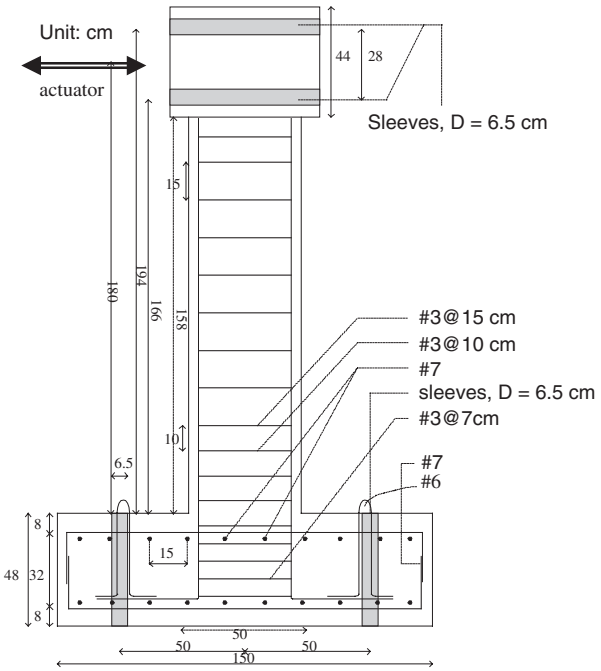

Figure 1. Layout of test RC columns.

superstructure) are 1.8 m and 323.7 kN, respectively. Its design spectrum is the displacement response spectrum derived from an artificial earthquake (Figure 2(a)) whose acceleration spectrum of 5% damping ratio is compatible with the design spectrum of the Taiwan Building Code for Soil Type II with the peak ground acceleration (PGA) of 0.33 g. This artificial earthquake is used as the input ground motion of pseudo-dynamic tests in this study. The design story drift ratio is 1.5% under the design earthquake ($\approx$ 27 mm). The design yield stress and modulus of elasticity of reinforcement are $f_y = 412$ MPa and $E_s = 2.0 \times 10^5$ MPa, respectively.

Moreover, the design compression strength of concrete is 20.6 MPa. However, the actual concrete strength obtained from samples of standard cylinders is 31.9 MPa. According to the direct displacement-based design procedure [11], the cross-sectional area and the longitudinal reinforcement ratio (ρ) of these test columns are 46.3 cm $\times$ 38 cm and 0.0158, respectively. Diameters of flexural and shear reinforcement are 15.9 mm (#5) and 9.53 mm (#3), respectively. The thickness of the cover concrete is 3.0 cm.

EXPERIMENTAL RESULTS

Pseudo-dynamic tests

The pseudo-dynamic test is a combination of experiment and structural dynamic analysis. For a non-linear SDOF system subjected to earthquake ground accelerations ($\ddot{x}_g$), its equation of

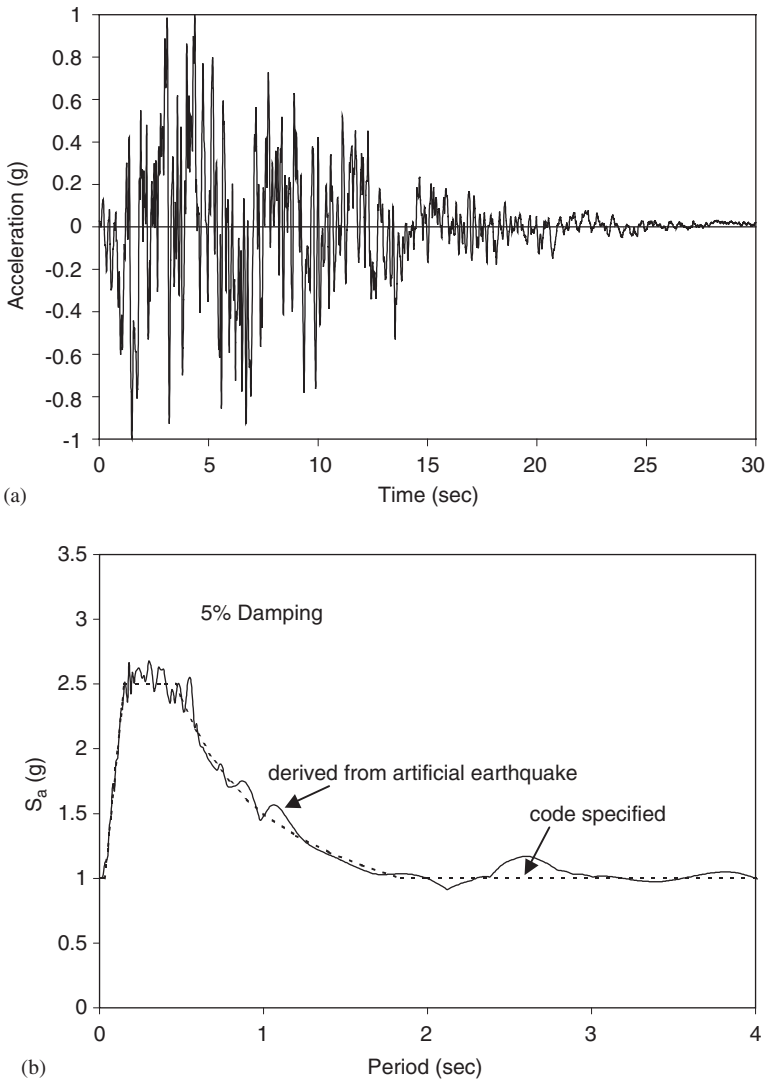

Figure 2. (a) Artificial earthquake for Soil Type II of TWA Building Code; and (b) normalised elastic acceleration response spectrum for Soil Type II of TWA Building Code.

motion can be expressed as

$$m\ddot{x} + c\dot{x} + r = -m\ddot{x}_g \tag{1}$$

where m, c and r are the mass, damping coefficient and restoring force of the system, respectively, and $\ddot{x}$ and $\dot{x}$ denote the relative acceleration and relative velocity of the mass. In a pseudo-dynamic test, values of the mass (m) and damping coefficient (c) are specified analytically. The ground motion acceleration ($\ddot{x}_g$) is also specified in the form of a digitised record while the restoring force (r) is obtained from experiment.

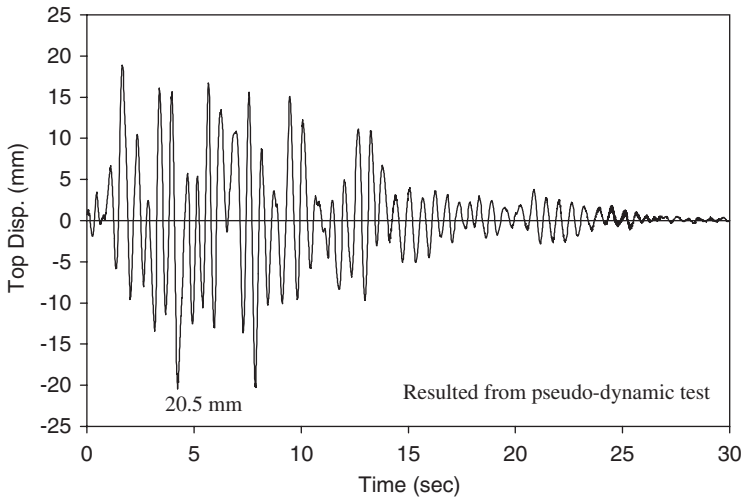

Figure 3. Displacement response of specimen I ($PGA = 0.33\,g$).

The pseudo-dynamic test is carried out in a series of time steps. In each step, the displacement (x_i) computed from Equation (1) is quasistatically applied to the test specimen by means of an electrohydraulic actuator. The restoring force (r) developed due to this deformation is measured at the end of the step by means of a load cell and is then substituted into Equation (1) to compute the displacement to be imposed in the next step (x_{i+1}). The equation of motion is solved using an explicit integration method such as the central difference method.

For the tests described in this paper, the mass of the specimens is taken to be equal to that of the supported structure plus 0.5 times the mass of the columns, and the viscous damping ratio is assumed to be 5% for the RC material. The intensity of input artificial earthquake ($\ddot{x}_g$, Figure 2(a)) for each specimen is $PGA = 0.33\,g$ (Specimen I), $0.36\,g$ (Specimen II) and $0.38\,g$ (Specimen III), respectively. Figure 3 shows the time history responses of top displacement (x) for Test Specimen I. The maximum displacement response of this specimen is 20.5 mm while that of the other two specimens is 23.5 mm (Specimen II) and 26.1 mm (Specimen III). These maximum values will be regarded as references for comparison with the evaluation results of the displacement coefficient method and the capacity spectrum method.

Pushover test

Because the surfaces of these test specimens are left almost without any damage after the pseudo-dynamic tests, the pushover test is immediately carried out on the Test Specimen I. Figure 4 represents the monotonic force–displacement relationship obtained from this specimen. It will be used as the pushover curve of the coefficient method and the capacity curve of the capacity spectrum method. Notice that this curve has been modified based on the results of the previous pseudo-dynamic test since this specimen had undergone slight yielding during that test. The work is done by comparing the force–displacement data of the pseudo-dynamic test with those of the pushover test. For a specified lateral force, the corresponding displacement responses are taken as the maximum one of both tests.

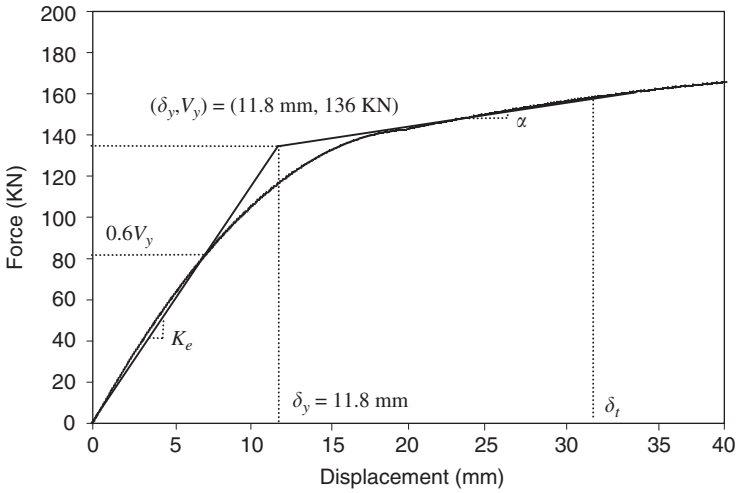

Figure 4. Pushover curve and its bilinear representation for test specimen I.

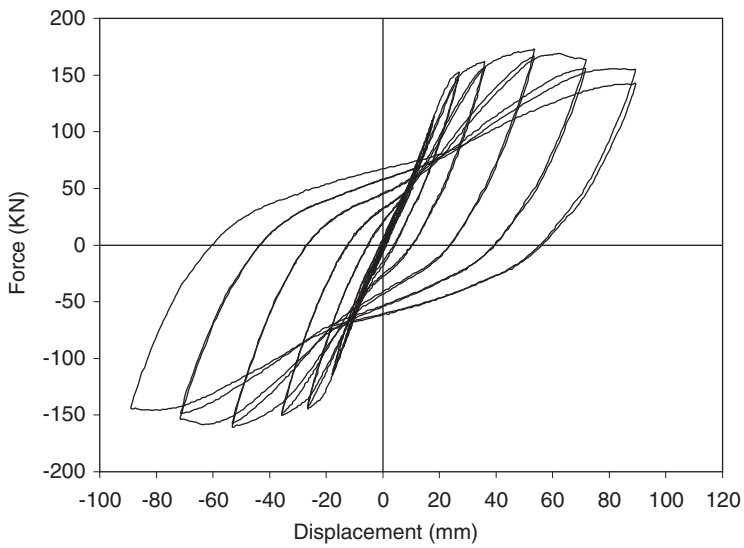

Figure 5. Results of cyclic loading tests.

Cyclic loading test

Figure 5 depicts hysterestic loops (force–displacement relationships) obtained from the cyclic loading test of Test Specimen II. In this figure, data within the linear range are unreliable because the test is conducted after the pseudo-dynamic test of this specimen. The purpose of showing the hysteretic loops is to see the level of strength and stiffness degrading of these RC columns. It is shown that these loops are very stable. The strength of this specimen still

increases and the degree of stiffness degrading is not obvious when displacement responses are less than 30 mm.

THE COEFFICIENT METHOD

According to the coefficient method of FEMA-273, the target displacement, which is the maximum displacement occurring at the top of structures during a chosen earthquake, can be determined as

$$\delta_t = C_0 C_1 C_2 C_3 S_a \frac{T_e^2}{4\pi^2} g \tag{2}$$

where C_0 = the differences of displacements between the control node of MDOF (multi-degree-of-freedom) buildings and equivalent SDOF systems; C_1 = the modification factor for estimating the maximum inelastic deformation of SDOF systems from their maximum elastic deformation; C_2 is the response to possible degradation of stiffness and energy dissipation capacity for structural members during earthquakes; C_3 = the modification factor for including the P–Δ effects; T_e = the effective periods of evaluated structures; and S_a = the spectral value of acceleration response corresponding to T_e.

In Equation (2), C_0 was derived from the participation factor of the first mode of structures as listed in Table I and C_1 was determined from Equation (3).

$$\begin{aligned} C_1 &= 1.0 && \text{for } T_e \geqslant T_0 \\ C_1 &= \frac{[1.0 + (R-1)T_0/T_e]}{R} && \text{for } T_e \leqslant T_0 \end{aligned} \tag{3}$$

where T_0 = characteristic periods of ground motions, and R = the ratio of required elastic strength to yield strength of structures. It can be computed as follows:

$$R = \frac{S_a}{V_y/W} \cdot \frac{1}{C_0} \tag{4}$$

where V_y = yield base shear derived from pushover analyses, and W = weight of structures. Moreover, Table II shows the values of C_2. The phenomena of stiffness and strength degrading easily happens to structures which have the properties of short period and low strength. With

Table I. Values for modification factor, C_0.

Number of stories	C_0
1	1.0
2	1.2
3	1.3
5	1.4
10+	1.5

Note: Linear interpolation should be used to calculate values.

Table II. Values for modification factor, C_2.

Performance level	$T_e = 0.1$ sec	$T_e > T_0$ sec
Immediate occupancy	1.0	1.0
Life safety	1.3	1.1
Collapse prevention	1.5	1.2

Note: For $0.1 < T < T_0$, linear interpolation should be used.

regard to C_3, when the ratio of post yield stiffness (α) is positive (>0), $C_3 = 1.0$. Otherwise, the following equation should be used.

$$C_3 = 1.0 + \frac{|\alpha|(R-1)^{3/2}}{T_e} \tag{5}$$

Results and comparisons

Because the test specimens are single-story structures, $C_0 = 1.0$ in accordance with Table I. The characteristic period of the ground motion (T_0) equals 0.465 sec for the design response spectrum of Soil Type II of the Taiwan Building Code. According to the pushover curve derived from the pushover test (Figure 4), the yield force (V_y) and effective stiffness (K_e) of the bilinearized force–displacement relationship (Figure 4) for Test Specimen I are 136 kN and 11.53 kN/mm, respectively. Consequently, the effective period becomes $T_e = 2\pi\sqrt{m/K_e} = 2\pi\sqrt{323.7/(11.53 \times 9810)} = 0.336$ sec; and, the spectral value of acceleration response corresponding to $T_e = 0.336$ sec and $PGA = 0.33\,g$ can be read from Figure 2(b) as $S_a = 0.33 \times 2.5 = 0.825$. Hence, according to Equations (4) and (3), R and C_1 can be computed as 1.96 and 1.19, respectively. In addition, $C_2 = 1.22$ for the case of life safety (Table II) and $C_3 = 1.0$ for a positive post-yield stiffness (Figure 4, $\alpha = 9.1\%$). Then, the target displacement (δ_t) of this specimen can be determined by Equation (2) as

$$\delta_t = C_0 C_1 C_2 C_3 S_a \frac{T_e^2}{4\pi^2}\, g = 1.0 \times 1.19 \times 1.22 \times 1.0 \times 0.825\, \frac{0.336^2}{4\pi^2} \times 9810 = 33.6\ \text{mm} \tag{6}$$

This value is sufficiently large. Since the degree of stiffness degrading of the column is not obvious (Figure 5), it can nearly be neglected under the design earthquake. Shown in Equation (7) is the target displacement which ignores the item of C_2.

$$\delta_t = C_0 C_1 C_3 S_a \frac{T_e^2}{4\pi^2}\, g = 1.0 \times 1.19 \times 1.0 \times 0.825\, \frac{0.336^2}{4\pi^2} \times 9810 = 27.5\ \text{mm} \tag{7}$$

Table III lists δ_t for these columns subjected to PGAs of $0.33\,g$, $0.36\,g$ and $0.38\,g$, respectively. Here, 'Exp.' represents the maximum top displacements measured from the pseudo-dynamic tests. From this table, it is clear that the coefficient method of FEMA-273 apparently overestimates the target displacements no matter what C_2 is used. The best result can be acquired if the effect of stiffness degrading of the column is neglected (i.e., set $C_2 = 1.0$ for the specimen). The average errors between 'Exp.' and the evaluated displacements are +54% for $C_2 = 1.22$ and +28% for $C_2 = 1.0$.

Table III. Target displacements evaluated by FEMA-273, (δ_t).

Design *PGA*	Exp. (mm)	δ_t (mm)	
		$C_0C_1C_2C_3S_a\frac{T_e^2}{4\pi^2}g$	$C_0C_1C_3S_a\frac{T_e^2}{4\pi^2}g$
0.33 *g*	20.5	33.6	27.5
0.36 *g*	23.5	36.7	30.0
0.38 *g*	26.1	38.7	31.7

Note: 'Exp.' = peak test top displacements obtained from pseudo-dynamic tests.

CAPACITY SPECTRUM METHOD – ADOPTED BY ATC-40

ATC-40 provides three different procedures (Procedures A, B and C) to estimate the earthquake-induced deformation demands (the target displacement or performance point), all based on the same principles but different from methods of implementation. In this study, only Procedure A is used. It is briefly described as follows.

1. Establish the relationship of base shear and roof displacement (i.e., capacity curve) of the evaluated structures by producing pushover analysis, and plot the 5%-damped elastic design response spectrum (i.e., demand curve).
2. Transfer both curves into the *A–D* format (Acceleration–Displacement) to obtain the capacity diagram and 5%-damped elastic demand diagram.
3. Choose an initial peak displacement (D_i) as the start point of iterations. Generally the point can be $D_i = S_d(T_n, \xi = 5\%)$. where S_d = displacement response spectrum and T_n = natural period of vibration.
4. Bilinearize the capacity diagram according to the rule of equal energy between the capacity diagram and its bilinear representation.
5. Using Equations (8) and (9), the reduced demand diagram can be acquired.

$$SR_A = \frac{3.21 - 0.68\ln(\beta_{eff})}{2.12} \tag{8}$$

$$SR_V = \frac{2.31 - 0.41\ln(\beta_{eff})}{1.65} \tag{9}$$

where SR_A and SR_V are the damping reduction factor for the ranges of constant acceleration and constant velocity, respectively. β_{eff} = the effective damping ratio computed by the following equations.

$$\beta_{eff} = \kappa\beta_0 + 0.05 \tag{10}$$

$$\beta_0 = \frac{1}{4\pi}\frac{E_D}{E_{So}} \leqslant 0.45 \tag{11}$$

where β_0 = the hysteretic damping ratio; E_D = the enclosed area of the bilinearized capacity diagram; and E_{So} = the maximum strain energy. The factor κ depends on the types of

Table IV. Iterative results and target displacements obtained from ATC-40, (D_u).

Design *PGA*	D_u (mm)	D_y (mm)	β_{eff}	SR_A	SR_V
0.33 *g*	17.0	4.6	0.21	0.53	0.64
0.36 *g*	18.9	5.1	0.24	0.50	0.62
0.38 *g*	19.9	5.5	0.25	0.48	0.60

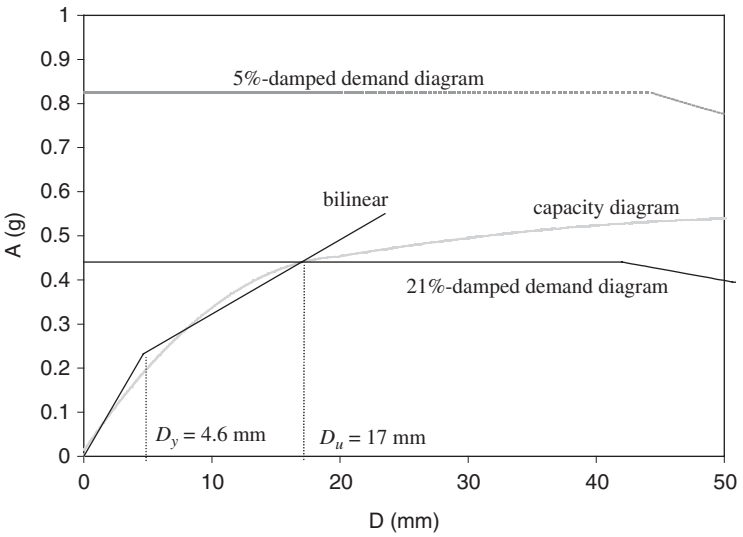

Figure 6. Capacity and demand diagram for test specimen I, $PGA = 0.33\,g$.

hysteretic behavior of the systems. Type A denotes hysteretic behavior with stable and full hysteresis loops. For such systems, $\kappa = 1$ if $\beta_0 \leqslant 16.25\%$, $\kappa = 0.77$ if $\beta_0 \geqslant 45\%$, and $\kappa =$ linear interpolation if $16.25\% \leqslant \beta_0 \leqslant 45\%$. Type C represents severely pinched loops; and the hysteretic behavior of the Type B system is between Type A and Type C.

6. Read-off the displacement D_{i+1} where the reduced demand diagram obtained from Step 5 intersects the bilinearized capacity diagram.
7. Check for convergence. If $(D_{i+1} - D_i) \div D_{i+1} \leqslant$ tolerance, the earthquake-induced deformation (target displacement) $D_u = D_{i+1}$. Otherwise, set $D_i = D_{i+1}$ (or another estimated value) and repeat Steps 4–7 until convergence.

Results and comparisons

In this study, the hysteretic behavior of the Type A system is used because the columns exhibited stable and full hysteresis loops (Figure 5) under the design earthquake. Table IV and Figure 6 show the iterative results based on the above-mentioned procedure. The target displacements for PGAs of 0.33 *g*, 0.36 *g* and 0.38 *g* are 17.0, 18.9 and 19.9 mm, respectively. These values are substantially smaller than those obtained from the pseudo-dynamic tests (20.5, 23.5 and 26.1 mm for $PGA = 0.33\,g$, $0.36\,g$ and $0.38\,g$, respectively). The reasons may result

Table V. Comparison of target displacements among 'exp. disp.', ATC-40 and Kowalsky damping model.

Design *PGA*	Exp. (mm)	ATC-40 (mm)	Kowalsky hysteretic damping model (mm)					
			$n=0$	$n=0.1$	$n=0.2$	$n=0.3$	$n=0.4$	$n=0.5$
0.33 *g*	20.5	17.0	17.6	19.6	22.1	25.1	29.1	35.2
0.36 *g*	23.5	18.9	21.3	23.4	26.0	29.7	34.9	41.5
0.38 *g*	26.1	19.9	23.9	26.4	29.4	33.3	39.3	48.4

Note: 'Exp.' = top displacements obtained from pseudo-dynamic tests.

from the use of Equation (11). The hysteretic damping ratios (β_0) are overestimated. Table V compares the outcomes if the Kowalsky hysteretic damping model (Equation (12), [11]) with various stiffness degrading factors (n) is adopted instead of Equation (11).

$$\beta_0 = \frac{1}{\pi}\left[1 - \mu^n\left(\frac{1-\alpha}{\mu} + \alpha\right)\right] \tag{12}$$

where μ = the ductility ratio. It can be seen from Table V that even for the case of $n=0$ (disregard the stiffness degradation), the target displacements estimated by the Kowalsky hysteretic damping model are closer to the experimental values than those estimated by Equation (11). The best accuracy can be gained if stiffness degradation is slightly considered ($n=0.1$). The average differences between 'Exp.' and the evaluated displacements are: -20% for ATC-40, -11% for the Kowalsky model with $n=0$, and -1.2% for the Kowalsky model with $n=0.1$.

Notice that the curve in Figure 6 is essentially linear beyond 10 mm, yet the yield point (D_y) is shown at 4.6 mm according to the rule of equal energy between the bilinear representation and the actual capacity diagram. It is very different from that obtained from the method specified in FEMA-273 (Figure 4).

CAPACITY SPECTRUM METHOD – USING INELASTIC DESIGN SPECTRUM

In Step 5 of the above section, the non-linear behavior of structures is predicted by equivalent damping. Differing from that, Fajfar [8] and Chopra and Goel [9, 10] proposed methods which implemented the inelastic design spectrum as the demand diagram to improve the capacity spectrum method. The following illustrates the procedures used in this paper.

1. Get capacity curve of the evaluated structure and establish an inelastic design spectrum with an assumed ductility ratio μ_i.
2. Transfer both curves to the *A–D* format (Acceleration–Displacement) to obtain the capacity diagram and demand diagram.

   Because the relationship of $D = \left(\frac{T_n}{2\pi}\right)^2 A$ does not exist in the inelastic response spectrum (Chopra and Goel [9, 10]), the following equation needs to be used for constructing the demand diagram:

$$D_u = \mu \frac{1}{R_\mu}\left(\frac{T_n}{2\pi}\right)^2 A_{\xi=5\%} \tag{13}$$

where $A_{\xi=5\%}$ = the 5%-damped elastic acceleration response spectrum, and R_μ = the force reduction factor due to non-linear behavior of structures. Several studies [12–14] have been carried out to investigate the relationship between R_μ and μ. In this paper, the formula of Equation (14) proposed by Newmark and Hall [12] is used.

$$R_\mu = \begin{cases} 1 & T_n \leqslant 0.03 \text{ sec} \\ \sqrt{2\mu - 1} & 0.125 \leqslant T_n \leqslant 0.66\sqrt{2\mu - 1}/\mu \\ \mu & T_n \geqslant 0.66 \text{ sec} \end{cases} \tag{14}$$

where linear interpolations should be applied between the ranges of $0.03 \text{ sec} < T_n < 0.125 \text{ sec}$ and $0.66\sqrt{2\mu - 1}/\mu < T_n < 0.66$ sec.

3. The displacement at the intersection of the capacity diagram and the demand diagram is D_u.
4. Bilinearize the capacity diagram in accord with the relationship of equal energy to obtain the yield displacement D_y. Then, $\mu_{i+1} = D_u/D_y$.
5. When $\mu_{i+1} \cong \mu_i$, iterations terminate. D_u is the target displacement. Otherwise, set $u_i = u_{i+1}$ and repeat Steps (1)–(5) until convergence occurs.

It should be noted that although the inelastic design spectrum is used in the above procedure, iterations are also needed due to the method of determining the yield point (yield displacement D_y and yield force V_y) of the pushover curve. The point in ATC-40 is unknown and needs to be obtained by constructing a bilinear representation of the capacity diagram according to the rule of equal energy. This will relate to the target displacement D_u. Because D_u is also an unknown variable, iteration procedures are required in order to find the correct yield point. Details can be found from pages 8–13 of the ATC-40 document [2]. Differing from the equal energy rule, the FEMA-273 uses $0.6\,V_y$ to define the yield point (bilinear curve) of the pushover curve. If this rule is implemented for determining the D_y and V_y of the capacity diagram in the capacity spectrum method, target displacement of a system can be achieved without iterations when the inelastic design spectrum is used.

Results and comparisons

Table VI gives the iterative processes for the case of $PGA = 0.33\,g$. Moreover, iterative results of the target displacements for PGAs equal to $0.33\,g$, $0.36\,g$ and $0.38\,g$ are 19.9, 21.8 and 23.6 mm, respectively. These values are somewhat less than those obtained from the pseudo-dynamic tests (20.5, 23.5 and 26.1 mm for $PGA = 0.33\,g$, $0.36\,g$ and $0.38\,g$, respectively) but they are acceptable. The mean difference between 'Exp.' and the evaluated displacements is −6.6%. Table VII lists a detailed comparison of the target displacements derived from various methods, and their errors corresponding to the experimental results are given in Table VIII.

SUMMARY AND CONCLUSIONS

Both the coefficient method used by FEMA-273 and the capacity spectrum method adopted by ATC-40 are administered for rehabilitation and evaluation of existing structures. The target displacement of the coefficient method is determined from the elastic displacement spectrum by using a number of modification factors while that of the capacity spectrum method is

Table VI. Iterative processes for the capacity spectrum method using the inelastic design spectrum ($PGA = 0.33\ g$).

Iteration no.	μ_i	R_μ	D_u (mm)	μ_{i+1}
1	2	1.73	25.2	2.74
2	2.10	1.79	21.7	2.36
3	2.15	1.82	20.2	2.20
4	2.16	1.82	19.9	2.16

Table VII. Comparison of target displacements for various evaluation methods.

Design *PGA*	Exp. (mm)	FEMA-273 (mm)	ATC-40 (mm) (mm)	Kowalsky (mm)		Inelastic spectra (mm)
				$n = 0$	$n = 0.1$	
0.33 *g*	20.5	27.5	17.0	17.6	19.6	19.9
0.36 *g*	23.5	30.0	18.9	21.3	23.4	21.8
0.38 *g*	26.1	31.7	19.9	23.9	26.4	23.6

Note: 'Exp.' = top displacements obtained from pseudo-dynamic tests.

Table VIII. Errors corresponding to 'Exp' for various evaluation methods.

Design *PGA*	FEMA-273 (%)	ATC-40 (%)	Kowalsky (%)		Inelastic spectra (%)
			$n = 0$	$n = 0.1$	
0.33 *g*	34	−17	−14	−4.4	−2.9
0.36 *g*	28	−20	−9	0.4	−7.2
0.38 *g*	21	−24	−8	1.4	−9.6
Average	28	−20	−11	−1.2	−6.6

Note: '+' = overestimate; '−' = underestimate.

obtained from equivalent linear SDOF systems. The two methods are members of non-linear static procedures because the pushover curves of the analyzed structures should be established whilst producing these methods.

Experimental comparisons and studies on the accuracy of the coefficient method and the capacity spectrum method have been made in this paper. Target displacements determined by both methods are assessed by carrying out the pseudo-dynamic tests, cyclic loading tests and pushover tests of three reinforced concrete columns. In addition to the Kowalsky hysteretic damping model, a modified capacity spectrum method which is based on the use of inelastic design response spectra is also discussed in this study. In order to reduce the errors between analysis and experiments, the pushover curves acquired from the pushover tests are directly used as the capacity curves of these evaluation methods. In addition, it is shown from the cyclic loading tests that the level of stiffness degrading of these columns is very slight and can almost be neglected when they are subjected to the design earthquakes.

On the basis of these test specimens (Table VIII), it is seen that the coefficient method overestimates the target displacements with a mean error of 28% while the capacity spectrum method underestimates them with a mean error of 20%. However, if the Kowalsky hysteretic damping model is used in the capacity spectrum method instead of the original damping model,

the average error becomes -11% for the case of ignoring the effect of stiffness degrading ($n = 0$) and -1.2% for the case of slightly including the effect of it ($n = 0.1$). Furthermore, if the inelastic design spectrum is implemented in the capacity spectrum method instead of the elastic design spectrum, the mean error decreases to -6.6% which somewhat underestimates the experimental results, but still can be accepted.

An additional phenomenon is observed from this study. In ATC-40, the yield displacement (D_y) and yield force (V_y) obtained from the rule of equal energy (Figure 6) between the pushover curve and its bilinear representation is very different from those obtained from the rule of $0.6\,V_y$ of FEMA-273 (Figure 4). For these test columns, the D_y and V_y achieved from the latter seem more reasonable than those achieved from the former since the curve within 10 mm is essentially linear. The equal energy rule also leads to the need for iterations even if the inelastic design spectrum is used in the capacity spectrum method.

ACKNOWLEDGEMENTS

This study was sponsored by the National Science Council (NSC-90-2811-Z-002-003) and the Sinotech Engineering Consultant Inc. (Grant No. 6120) of Taiwan, R.O.C. The financial support to the writers is greatly acknowledged.

REFERENCES

1. Federal Emergency Management Agency (FEMA). *NEHRP Guidelines for the Seismic Rehabilitation of Buildings*. Report FEMA 273 (Guidelines) and Report 274 (Commentary), Washington, D.C., 1997.
2. Applied Technology Council (ATC). *Seismic Evaluation and Retrofit of Concrete Building. Rep. ATC-40*, Redwood City, California, 1996.
3. Freeman SA, Nicoletti JP, Tyrell JV. Evaluations of existing buildings for seismic risk—A case study of Puget Sound Naval Shipyard, Bremerton, Washington. *Proceedings of the 1st U.S. National Conference on Earthquake Engineering* 1975; 113–122.
4. Freeman SA. Prediction of response of concrete buildings to severe earthquake motion. *Publ. SP-55*, American Concrete Institute, Detroit, 589–605, 1978.
5. Deierlein GG, Hsieh SH. Seismic response of steel frames with semi-rigid connections using the capacity spectrum method. *Proceedings of the 4th U.S. National Conference on Earthquake Engineering*, vol. 2, 1990; 863–872.
6. Reinhorn AM, Li C, Constantinou MC. *Experimental and analytical investigations of seismic retrofit of structures with supplemental damping*. Report No. NCEER-95-0001, State University of New York at Buffalo, N.Y., 1995.
7. Freeman SA. Development and use of capacity spectrum method. Paper No. 269. *The 6th US National Conference on Earthquake Engineering/EERI*, Seattle, Washington, 31 May–4 June, 1998.
8. Fajfar P. Capacity spectrum method based on inelastic demand spectra. *Earthquake Engineering and Structural Dynamics* 1999; **28**:979–993.
9. Chopra AK, Goel RK. *Capacity-demand-diagram methods for estimating seismic deformation of inelastic structures*: *SDF systems*. Report No. PEER-1999/02, Pacific Earthquake Engineering Research Center, University of California, Berkeley, CA, 1999.
10. Chopra AK, Goel RK. Evaluation of NSP to estimate seismic deformation: SDF systems. *Journal of Structural Engineering* (ASCE) 2000; **126**:482–490.
11. Kowalsky MJ, Priestley MJN, MacRae GA. *Displacement-based design*, *a methodology for seismic design applied to sdof reinforced concrete structures*. Report SSRP-94/16, Structural System Research Project, University of California, San Diego, La Jolla, California, 1994.
12. Newmark NM, Hall WJ. *Earthquake Spectra and Design*. EERI Monograph Series, Earthquake Engineering Research Institute, Oakland, California, 1982.
13. Miranda E, Bertero VV. Evaluation of strength reduction factor for earthquake resistant design. *Earthquake Spectra* 1994; **10**:357–379.
14. Applied Technology Council (ATC). *Structural Response Modification Factors. Rep. ATC-19*, Redwood City, California, 1995.

